

# Fully Automated Generation of Arteriogram and Venogram Using Correlation and Pooled Covariance Matrix Analysis

J. Du<sup>1</sup>, A. Karami<sup>1</sup>, Y. Wu<sup>2</sup>, F. Korosec<sup>2</sup>, T. Grist<sup>2</sup>, and C. Mistretta<sup>2</sup>

<sup>1</sup>Radiology, University of California, San Diego, CA, United States, <sup>2</sup>Medical Physics and Radiology, University of Wisconsin, Madison, WI, United States

**Introduction:** Time-resolved CE-MRA provides contrast dynamics in the vasculature. The temporal information can be further used to separate arteries from veins using a variety of algorithms such as correlation analysis (1), matched filtering (2), eigenimage filtering (3), feature space analysis (4), or Mahalanobis distance analysis (5). The ability to separate arteries from veins allows extended acquisition at the steady state as well as matched filtering of the whole data to improve both spatial resolution and signal to noise ratio (SNR). However, most of the segmentation algorithms require operator intervention such as thresholding. Improper thresholding may significantly reduce the image quality. Furthermore, the contrast dynamics pattern may vary significantly within a large coronal imaging field of view (FOV) due to delayed or asymmetric filling, or slow blood flow in the tortuous vessels (6). Correlation with single arterial and/or venous reference curves may result in misclassification. A single global thresholding of the correlation coefficients or Mahalanobis distance may not work well. Here we present a fully automated region-specific segmentation algorithm for effective separation of arteries from veins based on cross correlation and pooled covariance matrix analysis.

**METHODS:** The fully automated vessel segmentation algorithm shown in Figure 1 includes the following five steps: (i) Automated region-specific regions of interest (ROIs) for artery, vein and background are generated using an iterative thresholding algorithm based on the contrast arrival time map and contrast enhancement map. (ii) Region-specific matched filtering is performed for each region to optimize SNR for artery and vein, respectively. (iii) Region-specific cross correlation ( $CC_{k,REF}^j$ ) is performed for each voxel  $k$  from region  $j$  by correlating its time course to the arterial (A), venous (V) and background (B) reference curves, respectively. (iv) Region-specific pooled covariance matrix analysis is performed in the 3D feature space, where each voxel  $k$  from region  $j$  forms a cross correlation vector  $CC_k^j = (CC_{k,A}^j, CC_{k,V}^j, CC_{k,B}^j)$ . The mean correlation vector for region  $j$  is denoted as  $m^j$ . A  $3 \times 3$  variance matrix  $\Omega^j$  for region  $j$  is given by equation [1] where  $N_{REF}$  is the size of ROI. Pooled sample covariance matrix for region  $j$ ,  $\Omega^j(P)$  is the normalization of multiple-feature covariance matrix. Automated processing is performed by calculating the Mahalanobis distance (MD), which is a statistical distance measurement that accounts for the widths of the reference correlation coefficients distributions of each voxel relative to the arterial, venous and background peaks. The pooled MD of voxel  $k$  from region  $j$  relative to each feature is estimated using equation [2]. Voxel  $k$  is automatically allocated to the group with the smallest MD. (v) Formation of the composite images where the segmented low resolution dynamic image data are combined with the unsegmented matched filtered high resolution data in k-space

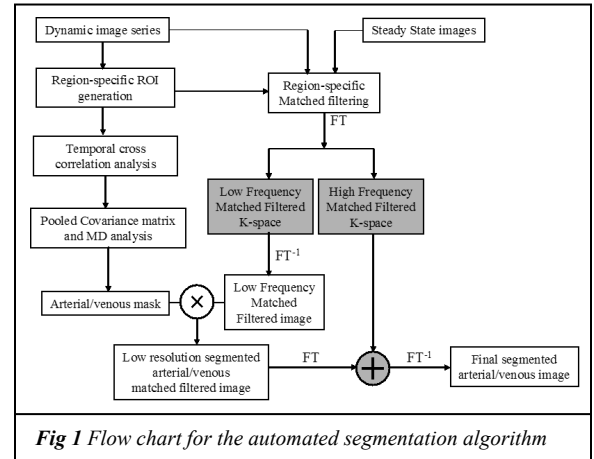


Fig 1 Flow chart for the automated segmentation algorithm

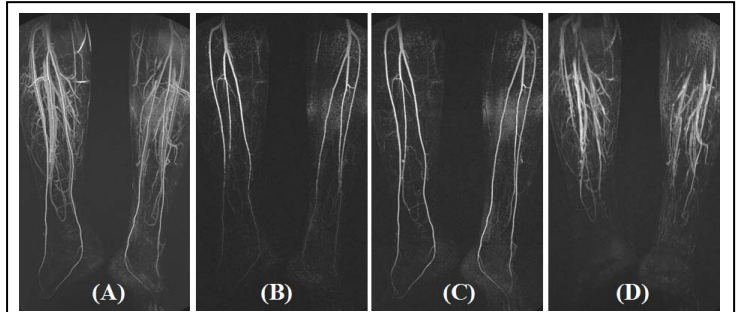


Fig 2 The matched filtered image (A), segmented images with global ROIs (B) and region-specific ROIs for artery (C) and vein (D) of a volunteer.

$$\Omega^j = \frac{1}{N_{REF} - 1} \sum_{l=1}^{N_{REF}} \left( \overline{CC_l^j} - \overline{m^j} \right) \left( \overline{CC_l^j} - \overline{m^j} \right)^T \quad (1)$$

$$MD_k^j = \left( \overline{CC_k^j} - \overline{m^j} \right)^T \Omega^j(P)^{-1} \left( \overline{CC_k^j} - \overline{m^j} \right) \quad (2)$$

and inverse Fourier transformed back to form the final segmented arterial and venous images. This algorithm was applied to 7 volunteer and patient studies acquired with a PR-HyerTRICKS sequence with a FOV of 44 cm, readout matrix of 512, 72 slices, slice thickness of 1.0 mm, TR/TE/flip angle = 7.4 ms/2.6 ms/30°. The total acquisition time was 3 min 58 seconds during which 24 time frames were acquired, with the first 82 seconds for mask data acquisition and the last 58 seconds for high frequency slice data acquisition.

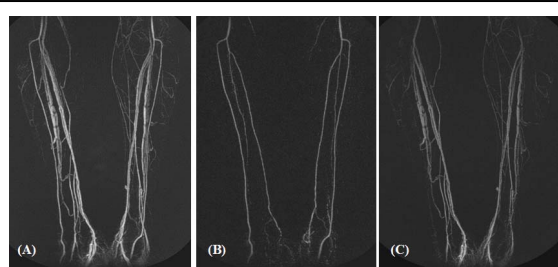


Fig 3 The matched filtered image (A), the segmented arterial image (B) and venous image (C) of a patient.

**RESULTS:** Figure 2 shows a volunteer study with region-specific matched filtering (Fig 2A) and a global correlation analysis (Fig 2B), as well as the automatically segmented arteriogram (Fig 2C) and venogram (Fig 2D). CNR between artery and vein is increased from 3.6 for the matched filtered image to 54 for the segmented arteriogram and 46 for the segmented venogram. Figure 3 shows a patient study with matched filtering (Fig 3A) and segmented arteriogram (Fig 3B) and venogram (Fig 3C). CNR between artery and vein is increased from 1.8 for the matched filtered image to 24 for the segmented arteriogram and 29 for the segmented venogram. Figure 4 shows another patient study with matched filtering (Fig 4A, B) and the segmented arteriogram (Fig 4C, D) in the coronal and sagittal reprojection. The measured CNR between artery and vein increased from 1.3 for the matched filtered image to 16 for the segmented arterial image.

**CONCLUSIONS:** Fully automated vessel segmentation can be applied to time-resolved CE-MRA to generate 3D angiograms and venograms with high spatial resolution, high SNR and CNR with minimal high frequency venous/arterial and background signal contamination.

## REFERENCES

1. Bock M, et al., MRM 2000 ; 43 :481-487.
2. Wang Y, et al., MRM 1993 ; 30 :600-608.
3. Kaandorp DW, et al., MRM 1999 ; 42 :307-313.
4. Zadeh HS, MRM 1998 ; 40 :443-453.
5. Mazaheri Y, et al., JMRI 2002 ; 15 :291-301.
6. Hany TF, et al, Radiology 2001 ; 72 :221-226.

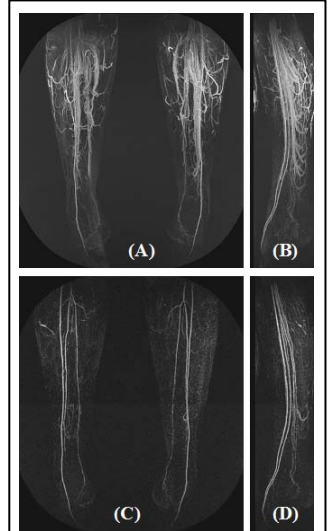


Fig 4 The matched filtered coronal (A) and sagittal (B) images and the segmented coronal (C) and sagittal (D) images of a patient.